The State Scientific Center of Russia
The Budker Institute of Nuclear Physics
SB RAS

V.S. Panin, S.V. Peleganchuk

RADIOACTIVITY AND ELECTRONIC NOISE IN LIQUID KRYPTON CALORIMETER

Budker INP 95-26

НОВОСИБИРСК

Radioactivity and Electronic Noise in Liquid Krypton Calorimeter

V.S.Panin, S.V.Peleganchuk

Abstract

The methods of calculation of electronic noise and radioactivity contributions to an energy resolution of ionization calorimeter based on liquid krypton are described. The results of calculations for LKr calorimeter of $KEDR$ detector are presented. The possibility of improvement of the resolution by means of multiply-sampled signals method is discussed.

The State Scientific Centre of Russia
The Budker Institute of Nuclear Physics, SB RAS

1. Introduction

The method of photons detection in a wide energy region by the ionization calorimeter based on liquid krypton (LKr) is developed at Budker Institute of Nuclear Physics during several years by a big group of authors. During this time the most of effects determining the space and energy resolution were analyzed, a several experiments with prototypes of calorimeter were performed. The LKr calorimeter of $KEDR$ detector for experiments in Υ-meson family at $VEPP-4M$ e^+e^- collider was designed and it is assembling at present time [1]-[9].

The main factors determining the energy resolution of the ionization LKr calorimeter at the moderate ($< 100MeV$) energies are the thermal noise of the electronics, radioactivity of krypton and geometric factor. The last is connected to the dependence of the response of ionization chamber on the distribution of the deposited energy inside the gap. All these effects can be calculated of course by traditional methods of Monte Carlo simulation, but the obtaining of good accuracy requires a lot of computing time, and the development of the analytical approach is interesting especially for the stage of a calorimeter design.

In the present note, the method of calculation of the electronic noise and radioactivity taking into account a finite life time of electrons in liquid due to their capture by electronegative impurities is described. The main formulae are given for the references and some specific results are presented for illustration. The method of geometric factor calculation was developed in ref.[10].

The described methods allow to minimize easy the contribution of these effects to the energy resolution.

Moreover, the possibility of resolution improvement by means of multiply-sampled signals method is discussed and the results of some specific calculations are presented.

2. Waveform of the useful signal

The electromagnetic LKr calorimeter of $KEDR$ detector consists of ionization chambers with the anode – cathode gap of 2 cm width with thin electrodes maid of foiled fiberglass ($G10$) and it is practically homogenous. Its energy resolution is comparable with the resolution of the best calorimeters based on heavy scintillation crystals when the electronics with a sufficiently small noise level is used. The space resolution for high energy photons is considerably better due to the possibility of measuring the coordinates of the photon conversion point in a special stripped structure located in the first 5 radiation lengths of the calorimeter. The read out electrodes are divided into rectangular pads, forming towers oriented to the interaction point.

Since the drift velocity of electrons in the field $\sim 1\ kV/cm$ is for several order of magnitude higher than that of ions, the ionization chambers are operated in an electron-pulse mode with a typical electron drift time of $\sim 10\ \mu s$. A charged particle crossing the gap of chamber produces the ionization with more or less uniform charge distribution inside the gap therefore the current waveform has a typical triangular shape. The inevitable presence of electronegative impurities in LKr lead to the capture of a part of electrons during a drift that is convenient to describe as a life time of electrons. The current pulses for three values of life time are shown in fig. 1(a).

When the shower producing particles (electrons or gamma-quanta) are detected, one can assume in a reasonable approximation that the energy in the calorimeter is deposited mainly by charged particles crossing the gaps of ionization chambers. Thus the useful signal has in average a triangular shape.

The fluctuations of the waveform are known as a geometric factor contributing to an energy resolution. Its value can be calculated by Monte Carlo method or, as it was shown in ref.[10], evaluated analytically.

Each tower of the calorimeter is connected to its own read out channel consisting of the charge sensitive preamplifier (CSP), shaper minimizing

noise-to-signal ratio and amplitude-to-digit converter (ADC) operating in peak sensitive mode. To measure the absorbed energy of the shower it is necessary to sum the pulse heights from several adjacent towers, and their number depends on the energy.

As far as signal processing is concerned, the CSP is equivalent to the integration cell with a time constant of several hundreds of microseconds. As a shaper for LKr calorimeter of $KEDR$ detector is used a symmetric $RC-2CR$ (one integration and 2 differentiations) chain of three independent cells. So the most of the specific calculations were performed for this type of shaper, although some more general cases are also considered.

The waveform of the signal at the input of ADC can be obtained by method of Laplace transformation for the shaper with arbitrary number of RC and CR cells, but the expression is rather cumbersome to present it here. The formulae for $RC-CR$, $RC-2CR$ and $2RC-CR$ shapers are given in appendix. The waveforms of useful signal for these shapers are shown in fig. 1(b-d) for different values of the life time of electrons and the time constant equal to 1/10 of a drift time.

3. Electronic noise

For practical estimation of the contribution of electronic thermal noise to the energy resolution of the calorimeter it is convenient to use the equivalent noise charge (Q_N) measured for the chosen shaper with the proper detector capacitance. However, Q_N measured for one type of shaper can be recalculated to another one with a sufficient accuracy.

Although in the practical importance cases the main contribution is given by the series noise, let us present more general formulae taking into account the parallel noise too.

As it is well known [11], Q_N reduced to the input of CSP is determined by the following way:

$$Q_N^2 = 2kT/R_p \cdot K_p + 2kTR_sK_s(C+C_0)^2,$$

where k is Boltzman constant, T–temperature, R_p and R_s are parallel and series noise resistances, C_0 is a "cool" capacitance of CSP, C–detector capacitance. K_p and K_s are so called parallel and series noise indices, determined by the following way:

$$K_p = \int_0^\infty h(t)^2 dt / h^2_{max}, \quad K_s = \int_0^\infty h'(t)^2 dt / h'^2_{max},$$

where $h(t)$ is the response to δ-like current signal at the input of CSP.

The dimensionless values K_p/τ and $K_s\tau$ depends on the shaper type only (τ–time constant of the shaper) and are given in table 1.

Table 1. Noise indices of $RC-CR$-shapers

Shaper	$RC-CR$	$2RC-CR$	$RC-2CR$
K_p/τ	1.847	2.559	1.175
$K_s\tau$	1.847	0.853	3.526

The values of R_p, R_s and C_0 are obtained by fitting of the experimental dependence $Q_N^2(\tau)$ measured for several values of the detector capacitance.

As it was mentioned above, the main contribution at short time constants gives the series noise that is equivalent to the random consequence of δ-like signals at the input of shaper. In this case the equivalent noise charge is:

$$Q_N = Q_0 + Q' \cdot C,$$

where Q_0 and Q' for a given CSP depend on the shaper type only and are proportional to $\sqrt{K_s}$ that allows to do the simple recalculation from one shaper type to another.

The energy equivalent of the noise can be obtained by normalization of Q_N (in units of fundamental charge) to the maximum of useful signal corresponding to unit energy deposition:

$$\sigma(MeV) = Q_N \cdot \omega h_{max}/w_{max},$$

where $\omega = 20.5\ eV$ – mean energy necessary to produced one electron-ion pair in LKr, h_{max}, w_{max} – pulse height at the output of the shaper for unit charge at the input of CSP created by the δ-like and real current pulse respectively.

It is useful to note, that for short time constants $Q_N \sim 1/\sqrt{\tau}$, $w_{max} \sim \tau$ and hence $\sigma(MeV) \sim \tau^{-3/2}$.

4. Radioactivity

The industry supplied krypton contains a small fraction of the β-radioactive isotope ^{85}Kr with a half-life of 10.5 years and the bound energy 0.67 MeV [12]. The specific activity of LKr is $300-400\ Bq/cm^3$ [2, 13]. It leads to the appearance of a random consequence of current pulses at the input of CSP fluctuating on the magnitude and the duration effecting as an extra noise source.

Its contribution (σ_r) to the energy resolution corresponding to mean rate f of decays can be obtained by averaging of the square of the output pulse for β-decay over energy, point of decay and time after normalization to the maximum of useful signal for unit energy deposition:

$$\sigma_r(\tau_l, \tau) = \frac{1}{w_{max}(\tau_l, \tau)} \left\{ \frac{f\varepsilon^2}{T_d} \int_0^{T_d} dT_r \int_0^\infty r^2(t, \tau_l, \tau; T_r) dt \right\}^{1/2},$$

where $r(t, \tau_l, \tau; T_r)$ – the response to signal from β-decay with an unit energy deposition,

$w_{max}(\tau_l, \tau)$ – the maximum of the useful signal with an unit energy deposition,

T_d – electrons drift time,

τ_l – electrons life time,

τ – shaper time constant,

T_r – duration of the radioactive current pulse,

f – mean rate of β-decays,

$\varepsilon = 0.286\ MeV$ – rms energy of the β - decay of ^{85}Kr.

The typical volume of LKr corresponding to one channel in the tower structure of the calorimeter is 5000 cm^3 thus the rate of β-decays $f = (1.5 \div 2) \cdot 10^6$ Hz. The formulae for $r(t, \tau_l, \tau; T_r)$ and $w(t, \tau_l, \tau)$ are given in appendix. The contribution of the radioactivity increases with the time constant and at small one is approximately proportional to $\sqrt{\tau}$.

5. Geometric factor

Since the charge collected from the gap of ionization chamber depends not only on the deposited energy but on its distribution inside the gap, its value does fluctuate and contribute to an energy resolution. This effect is known as a geometric factor that depends on the fraction of the collected charge and decrease with decrease of the shaper time constant.

This effect can be simulated by means of Monte Carlo method by dividing the gaps into thin slices in such a way the drift time through which should be much shorter than time constant. This way is reliable enough but requires a lot of computing time.

The analytical approach developed in ref.[10] simplifies considerably the calculation of this effect. The results obtained for the $KEDR$ calorimeter are compared to each other in fig. 2. One can see from this figure that they are in a good agreement.

6. Time constant optimization

Since the contributions of radioactivity and geometric effect increase and the electronic noise decreases with the shaper time constant increase , the minimum of their common contribution exists obviously. The value of this minimum and its position on the time constant depends on the shaper type and the life time of electrons. It is interesting that the optimal life time is not infinite, i.e. some level of impurities improves the resolution.

The calculation of discussed effects was performed for the $KEDR$ calorimeter where CSP based on field-effect-transistor $SNJ1800D$ [4, 6] is used. The equivalent noise charge (Q_N) for this CSP was measured with $RC-CR$ shaper with time constant 3 μs [14] and in units of fundamental charge can be well approximated [15] by:

$Q_N = 1.4 \cdot (C(pF) + 550)$.

The recalculation of Q_N for other time constants and shaper types was performed by the method described above (item.3). The necessary initial data are given in table 2.

Table 2. Initial data for calculation of resolution

Energy of detected photon	(MeV)	100
Specific radioactivity of LKr	(Bq/cm^3)	300
Gap of ionization chamber	(cm)	2
Total drift time	(μs)	10
Tower electric capacitance	(pF)	500
LKr volume in a single tower	(cm^3)	5000
Number of summed towers		9

The electronic noise, radioactivity and geometric factor for $RC-CR$, $2RC-CR$ and $RC-2CR$ shapers for life time of 1 μs and ∞ at the photon energy

Table 3. Shaper $RC-CR$

$\tau, \mu s$	$t_{max}, \mu s$	h/S	N, MeV	R, MeV	$G, \%$	$(N+R)_9, \%$	$(N+R+G)_9, \%$
0.25	0.76	27.6	1.56	0.38	1.60	4.83	5.08
0.50	1.22	19.0	0.99	0.45	2.05	3.27	3.87
1.00	1.92	14.6	0.64	0.56	2.48	2.55	3.56
1.50	2.53	13.1	0.51	0.65	2.70	2.49	3.67
2.00	3.08	12.4	0.42	0.73	2.84	2.52	3.80
2.50	3.60	12.0	0.38	0.80	2.93	2.67	3.96

Table 4. Shaper $RC-2CR$

$\tau, \mu s$	$t_{max}, \mu s$	h/S	N, MeV	R, MeV	$G, \%$	$(N+R)_9, \%$	$(N+R+G)_9, \%$
0.25	0.41	44.7	3.43	0.28	1.02	10.32	10.36
0.50	0.73	27.3	1.92	0.37	1.50	5.85	6.05
1.00	1.23	18.7	1.07	0.48	2.01	3.51	4.05
1.50	1.66	15.6	0.80	0.56	2.31	2.94	3.73
2.00	2.04	14.2	0.65	0.62	2.50	2.67	3.67
2.50	2.40	13.3	0.55	0.67	2.63	2.61	3.71

of 100 MeV are plotted versus time constant in figures 3-5.

More detailed information for life time of 1 μs is presented in tables 3-5, where

$\tau, \mu s$	–	time constant,
$t_{max}, \mu s$	–	time position of the peak of useful signal,
h/S	–	the ratio of pulse heights of δ-like and useful signals for the same input charge,
N, MeV	–	electronic noise for a single tower channel,
R, MeV	–	radioactivity for a single tower,
$G, \%$	–	geometric factor,
$(N+R)_9, \%$	–	common contribution of noise and radioactivity for sum of 9 towers,
$(N+R+G)_9, \%$	–	common contribution of all these sources for sum of 9 towers.

One can see from these data that the useful signal has a maximum at about 2 μs when the time constant is optimal. The common contribution of the discussed effects is $3.6 \div 3.8\%$ and is almost independent of the shaper type.

Table 5. Shaper $2RC-CR$

$\tau, \mu s$	$t_{max}, \mu s$	h/S	N, MeV	R, MeV	$G, \%$	$(N+R)_9, \%$	$(N+R+G)_9, \%$
0.25	1.04	22.3	1.06	0.40	1.79	3.39	3.84
0.50	1.75	16.1	0.71	0.49	2.27	2.58	3.43
1.00	2.90	13.1	0.48	0.62	2.69	2.34	3.57
1.50	3.98	12.1	0.38	0.74	2.89	2.49	3.81
2.00	5.00	11.7	0.31	0.83	3.00	2.67	4.02
2.50	6.00	11.5	0.29	0.92	3.07	2.91	4.23

The influence of electrons life time on the resolution is shown in a more detailed way in figures 6–8. One can see that optimal life time is $1 \div 2\ \mu s$. Resolution improvement compared to infinite life time is 20% for $RC-2CR$ shaper.

By chance the industry supplied krypton has a purity corresponding to the electrons life time close to optimum. However it is unknown what it will be at the real conditions in the calorimeter, so the presented data have rather approximate character.

The final choice of the shaper parameters should be done after filling the calorimeter by LKr and measuring its parameters – specific radioactivity, drift and life time of electrons and recombination coefficient. It will be necessary also to study situation with the pick up noise resulting in appearance of noise correlation in towers.

In the next items the possibility of multiply-sampled signals method for noise and radioactivity suppression is discussed.

7. Multiple samples method

The multiple samples method was developed for high luminosity facilities to suppress the *pile – up* noise connected with the random coincidences of the events from different collisions in ref.[16, 17]. After some modifications it can be used for suppression of common contribution of thermal noise and radioactivity for LKr calorimeter.

Let the waveform of signal is measured at n points forming the vector of measured values s_i $(i = 1, ..., n)$, and $w(t)$ is a response to an unit energy deposition. If the measurements are synchronized with signal formation and w_i – values of response at the same time points as s_i then $s_i = Aw_i$ with accuracy to noise, where A is an energy deposition. The value of A and estimation of its standard deviation σ_A one can find by minimizing the expression:

$$\chi^2 = \sum_{i,j}^{n} (s_i - Aw_i) V_{ij} (s_j - Aw_j) \equiv sVs - 2AwVs + A^2 wVw.$$

Here $sVs = \sum s_i V_{ij} s_j$, $wVs = \sum w_i V_{ij} s_j$, $wVw = \sum w_i V_{ij} w_j$, $V_{ij} = R_{ij}^{-1}$ and $R_{ij} \equiv R(t_i - t_j)$ – autocorrelation function of noise and radioactivity that will be defined below. The values of A and σ_A are:

$$A = \frac{wVs}{wVw}, \quad \sigma_A = \left[\frac{\partial^2 \chi^2}{\partial A^2}\right]^{-1} = \frac{1}{wVw}.$$

If the measurements are shifted by some δt one has to find two values – energy deposition A and delay time δt. It is convenient to introduce two parameters [16]: $\alpha_1 = A$ $\alpha_2 = A\delta t$, and to expand w into Taylor series around the points of measurements t_i:

$$w(t_i + \delta t) = w(t_i) + w'(t_i) \cdot \delta t.$$

Then χ^2 will be a function of α_1 and α_2:

$$\chi^2 = \sum_{i,j}^{n} (s_i - \alpha_1 w_i - \alpha_2 w_i') V_{ij} (s_j - \alpha_1 w_j - \alpha_2 w_j') \equiv$$

$$sVs - 2\alpha_1 wVs + \alpha_1^2 wVs + \alpha_1^2 wVw + \alpha_2^2 w'Vw' + 2\alpha_1\alpha_2 w'Vw - 2\alpha_2 w'Vs,$$

(denotes are obvious).

Solving the system of equations $\partial\chi^2/\partial\alpha_{1,2} = 0$, one finds α_1 and α_2:

$$\alpha_1 \equiv A = \frac{(wVs)(w'Vw') - (w'Vs)(w'Vw)}{\Delta},$$

$$\alpha_2 \equiv A\tau = \frac{(wVw)(w'Vs) - (w'Vw)(wVs)}{\Delta},$$

$$\Delta = (wVw)(w'Vw') - (w'Vw)^2$$

and the correlation matrix:

$$\rho_{ij} = \left[\frac{1}{2}\frac{\partial^2\chi^2}{\partial\alpha_i\partial\alpha_j}\right]^{-1} = \begin{pmatrix} wVw & w'Vw \\ w'Vw & w'Vw' \end{pmatrix}^{-1} = \frac{1}{\Delta}\begin{pmatrix} w'Vw' & -w'Vw \\ -w'Vw & wVw \end{pmatrix},$$

i.e. $\sigma_A^2 = w'Vw'/\Delta$, $\sigma_{A\tau}^2 = wVw/\Delta$.

8. Noise and radioactivity autocorrelation functions

Let σ_n,σ_r and σ are noise, radioactivity and their common contribution and $R_n(t)$, $R_r(t)$ and $R(t) = R_n(t) + R_r(t)$ are the corresponding autocorrelation functions.

Since a series noise gives a main contribution to the electronic noise, we consider this one only. Then autocorrelation function is:

$$R_n(t) = \sigma_n^2 \frac{\int_0^\infty h'(u+t)h'(u)du}{\int_0^\infty (h'(u))^2 du},$$

where $h'(t) = dh/dt$, $h(t)$ – the electronic response to δ-like current pulse. The formulae for $h(t)$ for various types of shapers are given in appendix.

Calculation of $R_r(t)$ can be done by averaging on the energy and point of β-decay like the calculation of σ_r, i.e.

$$R_r(t) = \sigma_r^2 \frac{\frac{1}{T_d}\int_0^{T_d} dT_r \int_0^\infty r(u+t;T_r)r(u;T_r)du}{\frac{1}{T_d}\int_0^{T_d} dT_r \int_0^\infty r(u,T_r)^2 du},$$

where $r(t,T_r)$ - response to signal from radioactivity of a duration T_r. The formulae for it are also in appendix.

It is possible to show that the double integrations in the last formula can be reduced to ordinary integrals of the response to useful signal, namely:

$$R_r(t) = \sigma_r^2 \frac{\int_0^\infty w(u+t)w(u)du}{\int_0^\infty w(u)^2 du}.$$

Use of this formula considerably saves the computing time in numerical

calculations.

9. Results of some specific calculations

Below are given some results of specific calculations performed by described method that are assumed to be compared to the experiment in the future.

The following values of initial parameters were taken: drift time $T_d = 10\ \mu s$, tower capacitance $C = 500\ pF$, tower volume $V = 5000\ cm^3$, electronic noise for $RC-2CR$-shaper $Q_N = 1.4\cdot(C+550)\cdot(3/\tau)^{1/2}\cdot 1.38$ (the last factor recalculates the noise from $RC-CR$ to $RC-2CR$ shaper.) The results for single measurement for two life times of electrons (τ_l) are shown in table 6. Time constant (τ) was chosen optimal respective to noise, radioactivity and geometric factor for 9 summing towers at photon energy $E_\gamma = 100\ MeV$.

Table 6. Resolution at a single measurement

τ_l, μs	τ, μs	N_9, %	R_9, %	$(N+R)_9$, %	G, %	S, %
1	2.3	1.95	1.96	2.76	2.58	3.78
10	0.9	2.61	1.86	3.21	3.26	4.58

Here N_9, R_9, $(N+R)_9$ – noise, radioactivity and their quadratic sum for 9 towers, G – geometric factor, S – resulting contribution of all three factors.

The results obtained by method of multiply samples are shown in the following figures. The waveform of useful signal (a), autocorrelation functions for noise, radioactivity and their weighted sum ($b-d$) are plotted in fig. 9. The noise and radioactivity versus the time interval between points of measurements are shown in fig. 10,11 for life time 10 and 1 μs. The time constant of shaper was fixed at the optimum value for a single measurement.

As one can see from these figures at long life time ($\tau_l = 10\ \mu s$) the relative improvement of noise and radioactivity with 9 samples and the interval $\delta_t \approx 0.3\ \mu s$ is about 30% compared to a single measurement with an absolute value of $0.8 MeV$ for single tower. An increase of the number of points rather slightly improves the result. At the short life time ($\tau_l = 1\ \mu s$) the relative improvement is considerably less while absolute value is practically the same as one at $\tau_l = 10\ \mu s$.

The results for 1 and 9 measurements are shown as function of time constant in fig. 12,13 when the time interval between samples was optimized for each value of time constant. One can see from this figures that the common noise and radioactivity contribution slightly depends on the time constant in a wide region and is considerably improved compared to the single measurement especially for short time constants. It allows to hope that the geometric factor also can be considerably suppressed but this question needs an additional study.

10. Conclusions

The described methods give the simple possibility for estimations of noise, radioactivity and geometric effect contribution to an energy resolution of ionization LKr calorimeter as well as for optimization of electrode structure and electronic channel for single measurement by peak ADC. For the $KEDR$ calorimeter, in particular, was found the optimum of electrons life time $\approx 1\ \mu s$ at the drift time 10 μs.

The possibility of noise and radioactivity improvement by multiply samples method has been studied and improvement of $\approx 30\%$ was found for situation close to the $KEDR$ LKr calorimeter.

In conclusion the authors express their sincere gratitude to V.M.Aulchenko, S.G.Klimenko, A.P.Onuchin and Yu.A.Tikhonov for the interest to work and useful discussions.

The work is partially supported by Russian Foundation of Fundamental Researches, grant N 94-02-03995.

A Appendix

Here are given for references the formulae omitted for brevity in the main text.

A.1 Response to a δ-like current at the input of CSP

The input current $I = Q_0 \cdot \delta(t)$ is transformed by CSP with an equivalent capacitance C_0 into a step of power (neglecting difference between CSP time constant and infinity) $U_0(t) = Q_0/C_0 \equiv U_0 \cdot \theta(t)$ ($\theta(t) = 1$ for $t > 0$ and 0 otherwise) being the input signal for the shaper.

The Laplace transformations at the input of shaper is $U_0(p) = U_0/p$. The transformations after integrating (RC) and differentiating (CR) cells with time constant $\tau = RC = 1/p_0$ are obtained by multiplication by $p_0/(p+p_0)$ and $p/(p+p_0)$ respectively.

For three simplest kinds of shaper the response functions for $U_0 = 1$ are:
$h_{11}(x) = x \cdot exp(-x)$ for $RC - CR$,
$h_{21}(x) = \frac{1}{2}x^2 \cdot exp(-x)$ for $2RC - CR$
$h_{12}(x) = x(1 - x/2) \cdot exp(-x)$ for $RC - 2CR$-shaper; $x = t/\tau$

Obliviously, $h_{12} = h_{11} - h_{21}$. Peaking times (x_{max}) of these functions are given in table A1.

Table A1

Shaper	$RC - CR$	$2RC - CR$	$RC - 2CR$
x_{max}	1	2	$2 - \sqrt{2}$
h_{max}	$e^{-1} = .368$	$2e^{-2} = .271$	0.231

The response to any input current $I(t)$ is obtained by its convolution with function h:

$$U(t) = \int_0^t I(u)h(t-u)du = \int_0^t I(t-u)h(u)du$$

A.2 Response to 'rectangular' and 'triangular' current pulse

Neglecting a path of the electron from β-decay in liquid the corresponding current pulse for unitary produced charge can be written as:

$$I_r(t) = 1/T_d \cdot exp(-t/\tau_l), \quad 0 \le t \le T_r,$$

where T_d is a drift time, τ_l–life time of electrons, T_r–current duration determined by the point of β-decay in the gap of ionization chamber. When $\tau_l \to \infty$ the current has a step-like shape of duration T_r – 'rectangular' pulse.

Assuming useful signal to be produced by the particles crossing whole gap one has a current pulse for unit charge in the form:

$$I_s = \frac{1}{T_d} \cdot (1 - t/T_d) \cdot \exp(-t/\tau_l), \quad 0 \le t \le T_d$$

– 'triangular' pulse at infinite τ_l.

The formulae for signals after symmetric shapers are given below. Let τ is time constant,

$$\tau' = \tau_l\tau/(\tau_l - \tau), a = \tau'^2/(T_d\tau), x = t/\tau',$$

$$f(t) = exp(-t/\tau), \quad P_n(u) = -n! \sum_{k=0}^{n} u^k/k!,$$

$$x_{r,d} = \begin{cases} 0, & \text{if } t < T_{r,d} \\ (t - T_{r,d})/\tau', & \text{if } t \ge T_{r,d} \end{cases},$$

$$g_{r,d} = \begin{cases} exp(-t/\tau_l), & \text{if } t < T_{r,d} \\ exp\{-(t - T_{r,d})/\tau - T_{r,d}/\tau_l\}, & \text{if } t \ge T_{r,d} \end{cases}.$$

Then signals from radioactivity have the form:

$$r_{11}(t) = a\{f(t)P_1(x) - g_r(t)P_1(x_r)\},$$

$$r_{21}(t) = a\tau'/(2\tau)\{f(t)P_2(x) - g_r(t)P_2(x_r)\},$$

$$r_{12}(t) = r_{11}(t) - r_{21}(t),$$

and useful signals –

$$w_{11}(t) = a\{f(t)[P_1(x)(1 - t/T_d) + P_2(x)\tau'/T_d] -$$

$$g_d(t)[P_1(x_d)(1 - t/T_d) + P_2(x_d)\tau'/T_d]\},$$

$$w_{21}(t) = a\tau'/(2\tau)\{f(t)[P_2(x)(1 - t/T_d) + P_3(x)\tau'/T_d] -$$

$$g_d(t)[P_2(x_d)(1 - t/T_d) + P_3(x_d)\tau'/T_d]\},$$

$$w_{12}(t) = w_{11}(t) - w_{21}(t).$$

These formulae are convenient for computations at any reasonable region of parameters except of $\tau_l \simeq \tau$. This region requires an extra attention at computations.

References

[1] V.M.Aulchenko et al., Proc. of the 24 Int. Conf. on High Energy Physics, Munich, 1988 (contrib. paper); V.V.Anashin et al., Proc. of the Int. Symp. on Position Detect. in High Energy Physics, Dubna, 1988, p.58

[2] V.M.Aulchenko et al., Nucl.Instr.and Meth. A289 (1990) 468

[3] V.M.Aulchenko et al., Proc. of the 5th Int.Conf. on Instr. for Coll.Beam Phys., Novosibirsk, 1990, p.299,

[4] V.M.Aulchenko et al., Proc. Int.Conf. on Calorimetry at High Energy Physics, FNAL, 1990,

[5] V.M.Aulchenko et al., Proc. 4-th Topical Seminar on Exp. Apparatus for High Ener. Part. Phys. and Astrophys., San Miniato–1990

[6] P.Cantoni et al., Proc. Fifth Pisa Conf. on Calorimetry at High Energy Phys., Pisa-1991

[7] V.M.Aulchenko et al., Nucl.Instr.and Meth. A316 (1992) 8

[8] V.M.Aulchenko et al., Nucl.Instr.and Meth. A327 (1993) 194

[9] V.M.Aulchenko et al., XXVII Intern. Conf. on High Energy Physics, contributed paper gls0753, Glasgow, 1994

[10] V.I.Yurchenko, private communication

[11] V.Radeka, Ann. Rev. Nucl. Part. Sci. (1988) 38, 217-277

[12] Tables of Physical Values, p.834, Moscow, Atomizdat, 1976 (in russian)

[13] A.Gonidec, talk presented at Beijing calorimetry symposium, Beijing, 1994

[14] V.M.Aulchenko, L.A.Leontiev, private communication

[15] A.P.Onuchin, private communication

[16] W.E.Cleland and E.G.Stern, talk presented at the Corpus Christi Conference, Sept. 1992.

[17] N.Launay, C.de la Taille and L.Fayard, ATLAS Internal Note, CAL-NO-024, 12 July 1993

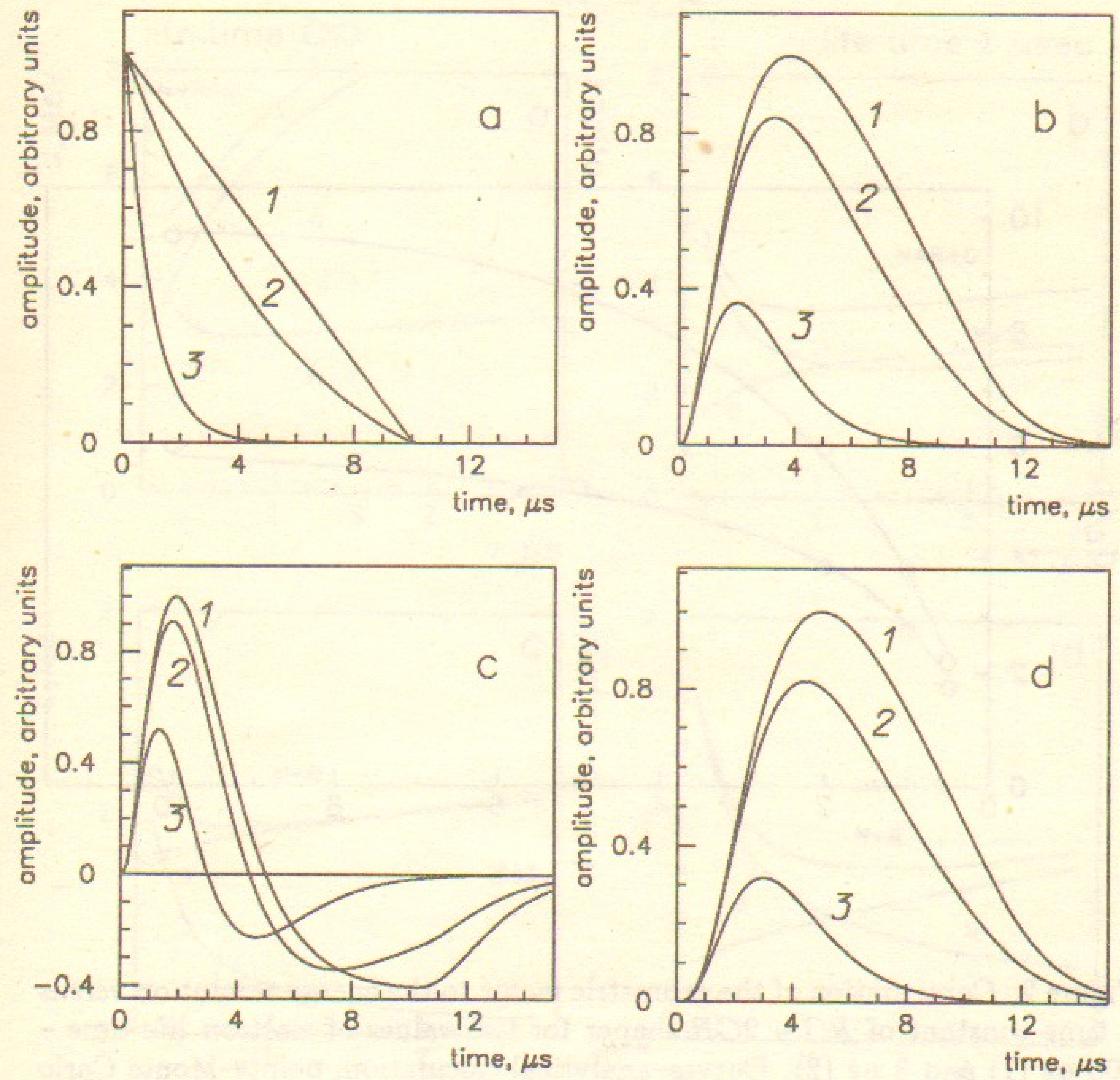

Figure 1. Current pulse (a) and waveform of the useful signal for electronics with $RC-CR$ (b), $RC-2CR$ (c) and $2RC-CR$ (d) shapers. An electron life time: 1–infinite, 2–10 μs, 3–1 μs.

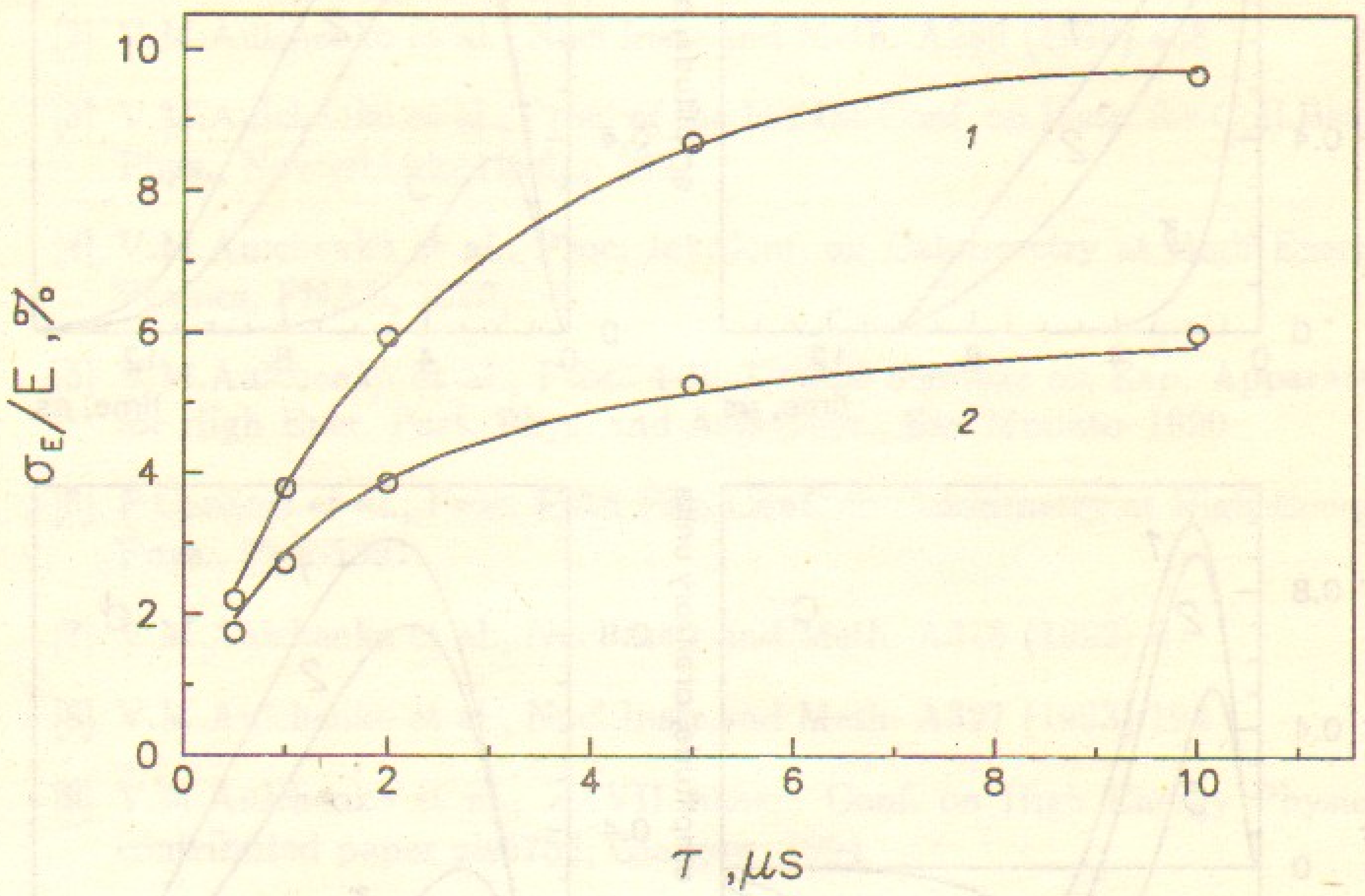

Figure 2. Contribution of the geometric factor to the energy resolution versus a time constant of $RC - 2CR$ shaper for two values of electron life time – 100 μs (1) and 3 μs (2). Curves–analytical calculation, points–Monte Carlo simulation results. A photon energy is 100 MeV.

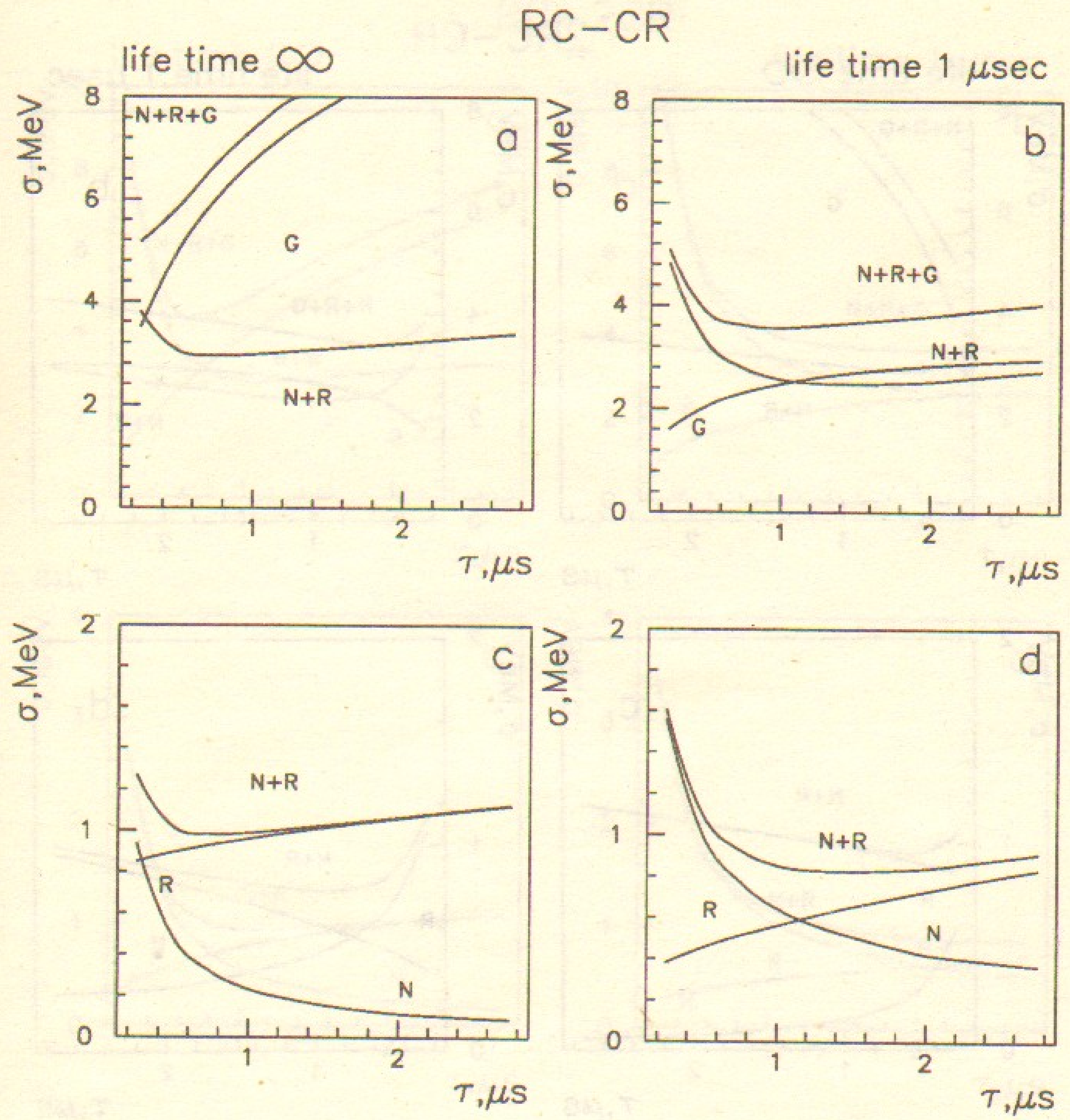

Figure 3. An electronic noise (N), radioactivity (R) and geometric factor (G) for $RC - CR$ shaper versus time constant. (a,c)–infinite electron life time, (b,d)–1 μs. (c,d)–N and R for one tower, (a,b)–N, R and G for sum of 9 towers.

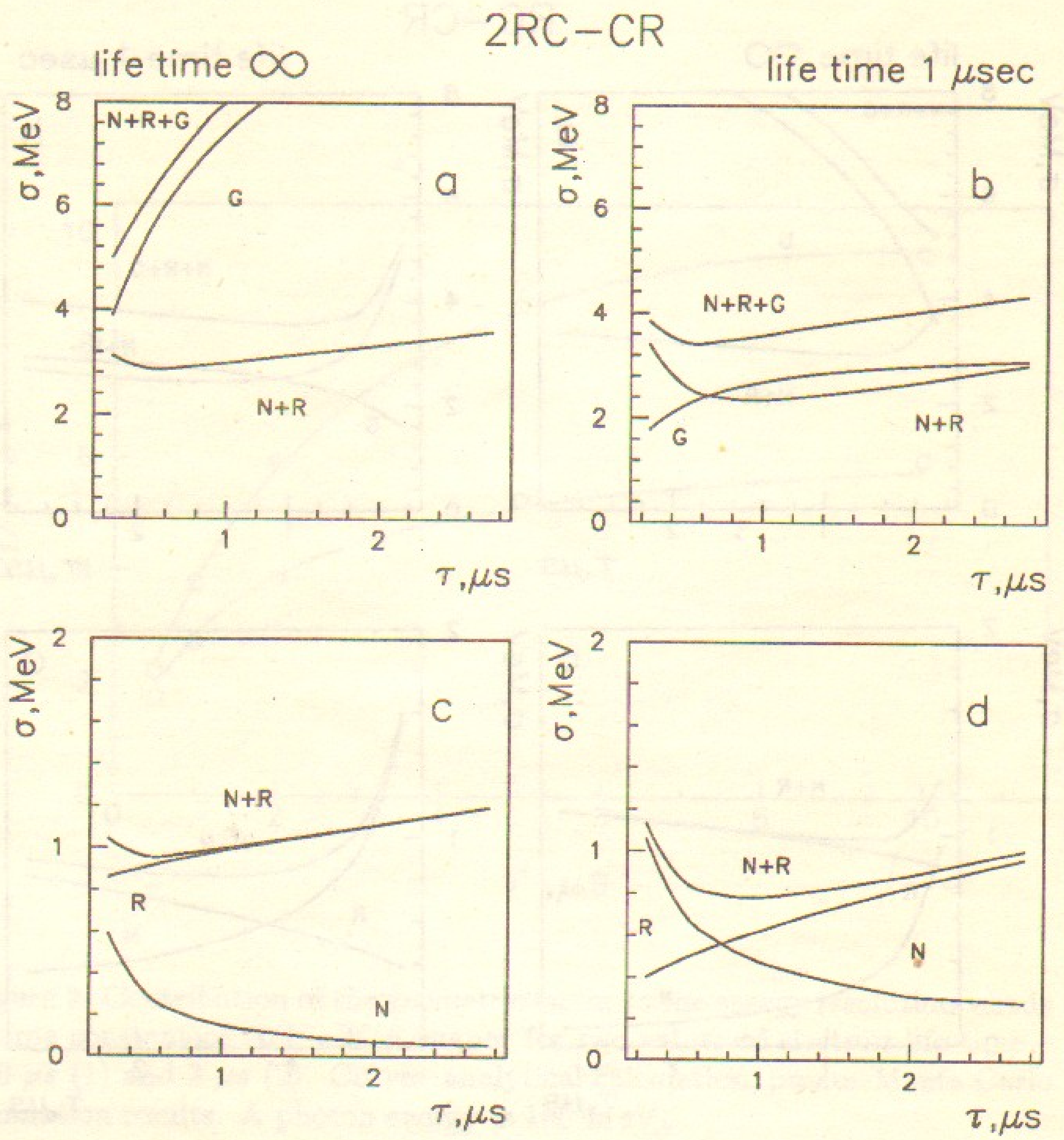

Figure 4. An electronic noise (N), radioactivity (R) and geometric factor (G) for $2RC - CR$ shaper versus time constant. (a,c)–infinite electron life time, (b,d)–1 μs. (c,d)–N and R for one tower, (a,b)–N, R and G for sum of 9 towers.

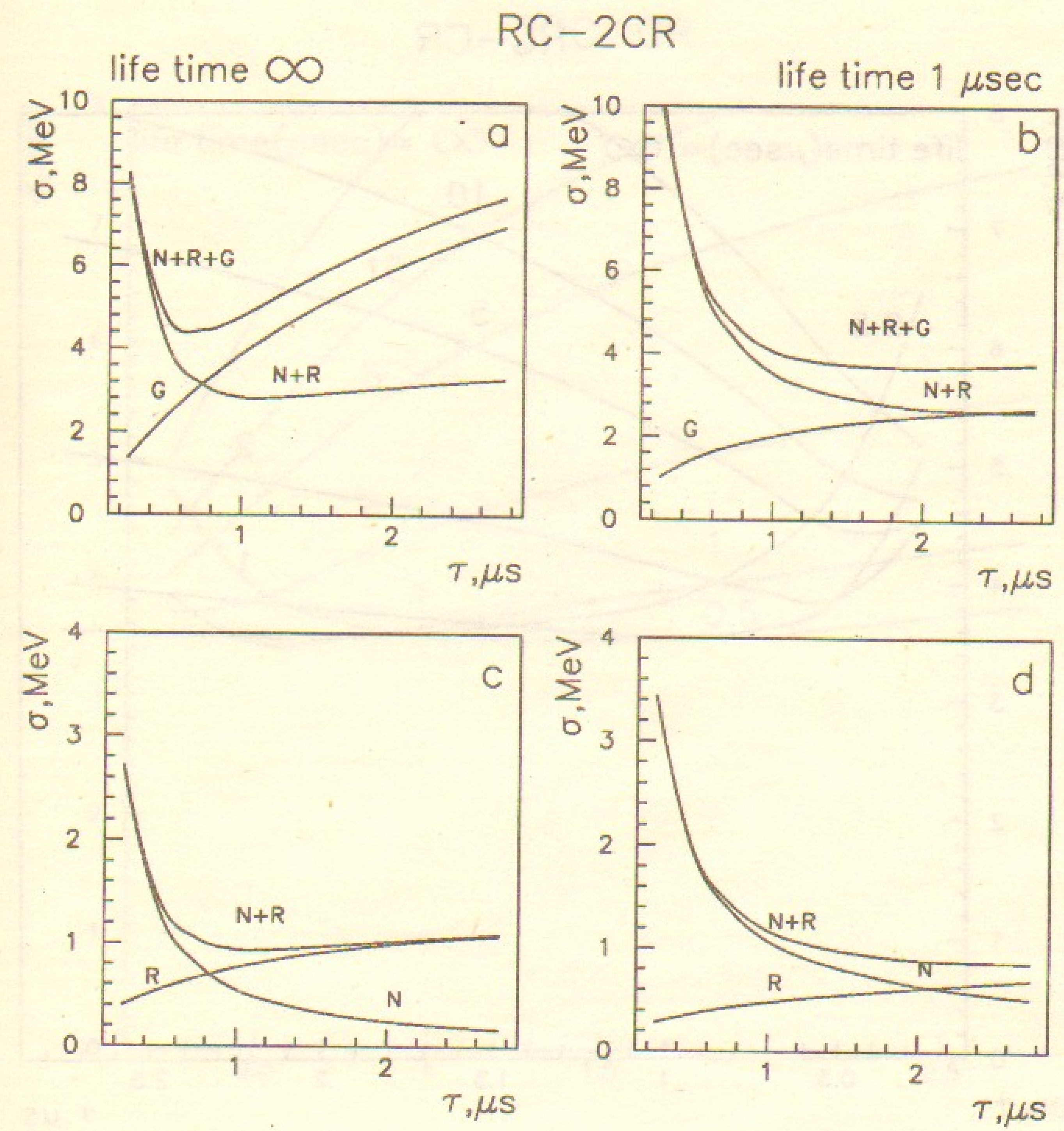

Figure 5. An electronic noise (N), radioactivity (R) and geometric factor (G) for $RC - 2CR$ shaper versus time constant. (a,c)–infinite electron life time, (b,d)–1 μs. (c,d)–N and R for one tower, (a,b)–N, R and G for sum of 9 towers.

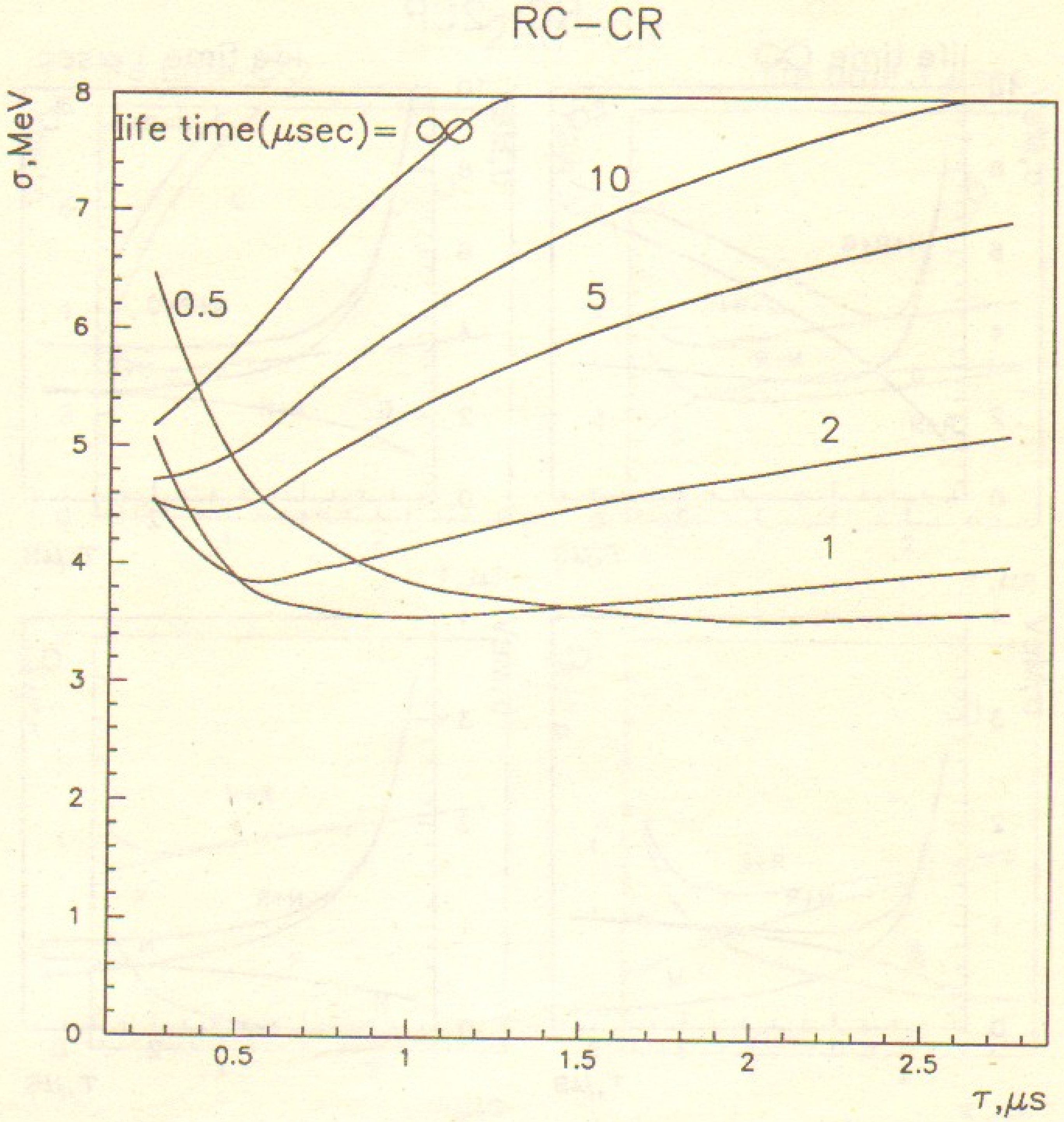

Figure 6. The sum of electronic noise, radioactivity and geometric factor for $RC-CR$ shaper versus time constant for a few electron life time (figure over curve). The results is for sum of 9 towers.

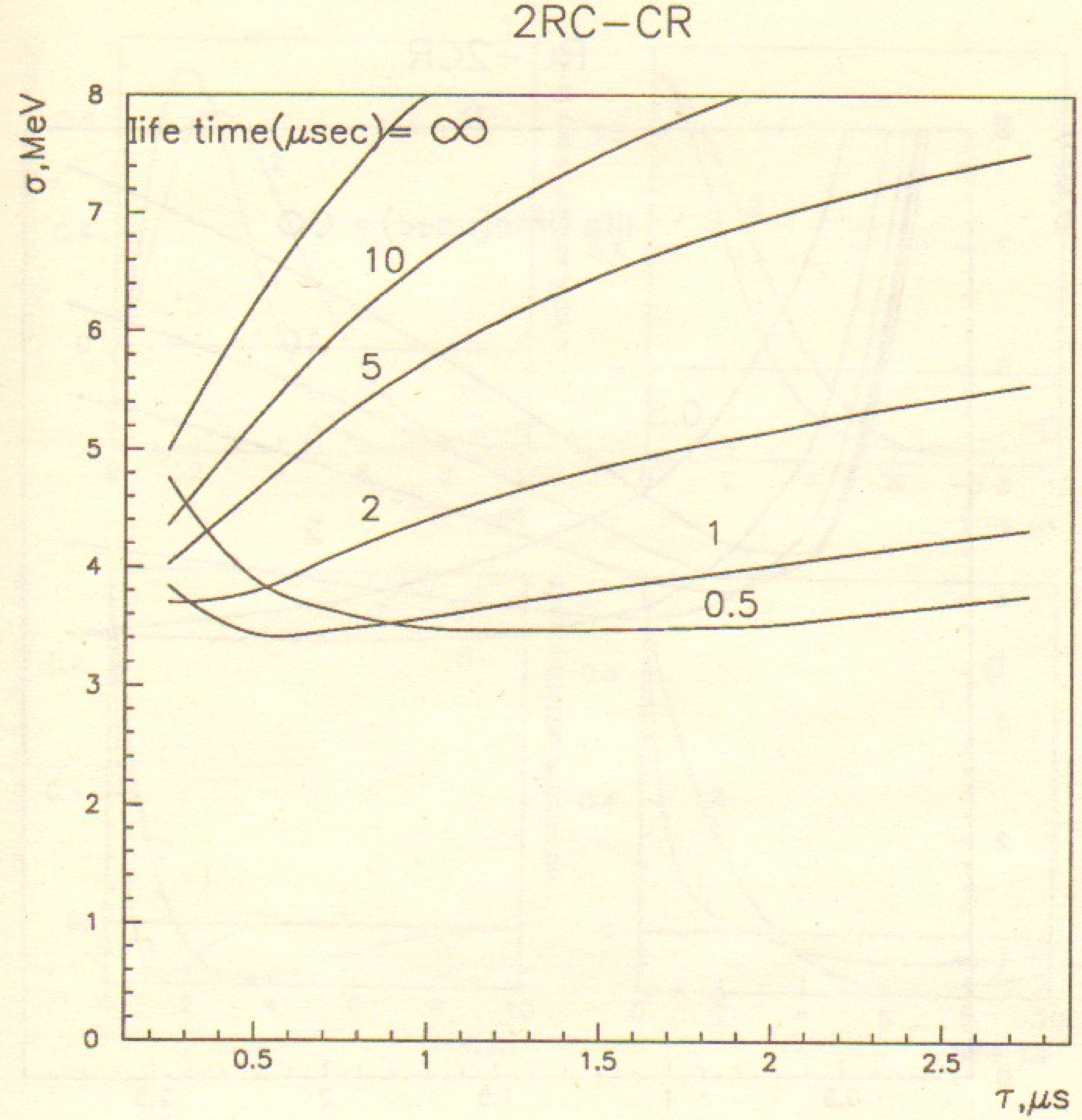

Figure 7. The sum of electronic noise, radioactivity and geometric factor for $2RC-CR$ shaper versus time constant for a few electron life time (figure over curve). The results is for sum of 9 towers.

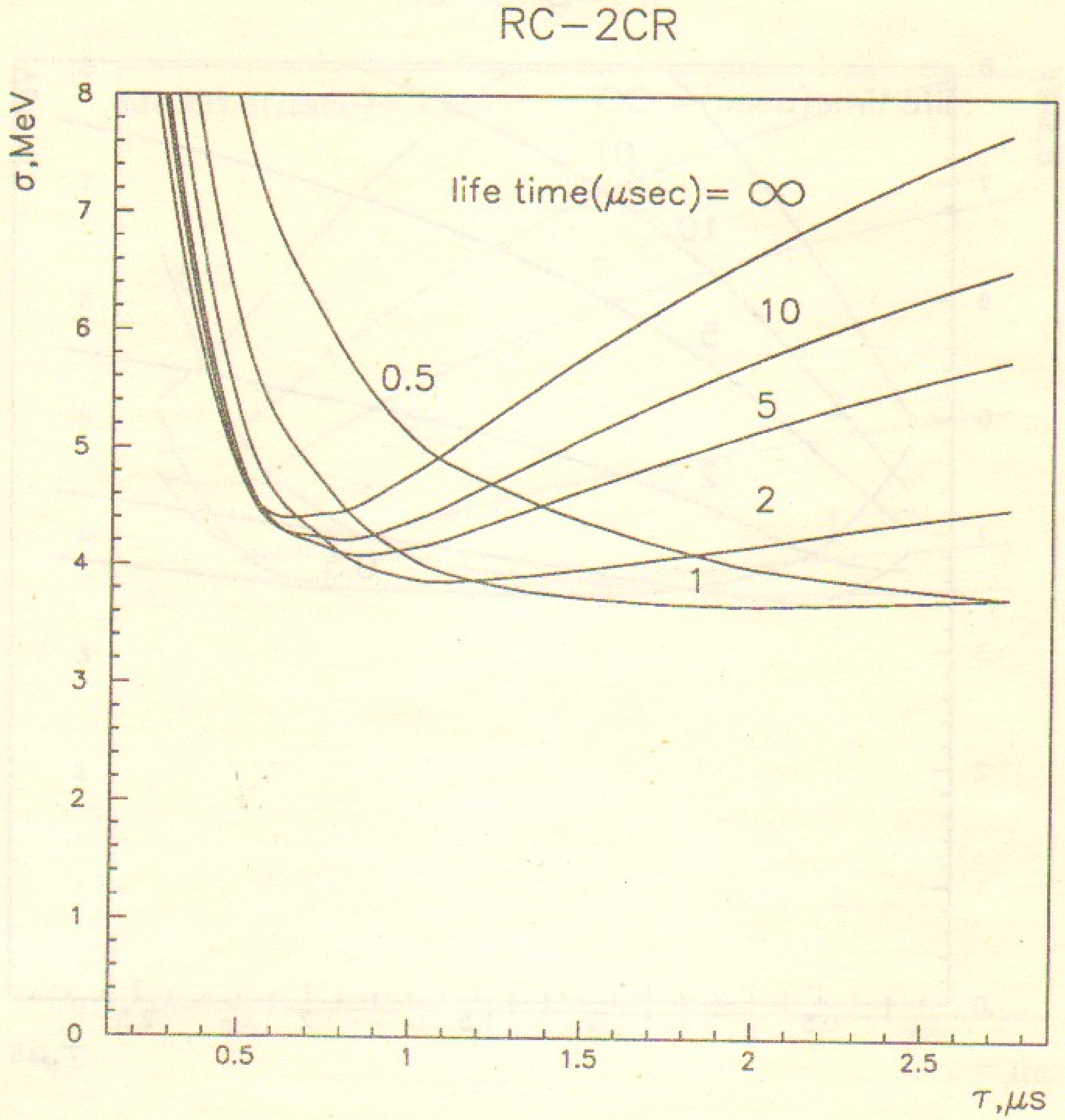

Figure 8. The sum of electronic noise, radioactivity and geometric factor for $RC-2CR$ shaper versus time constant for a few electron life time (figure over curve). The results is for sum of 9 towers.

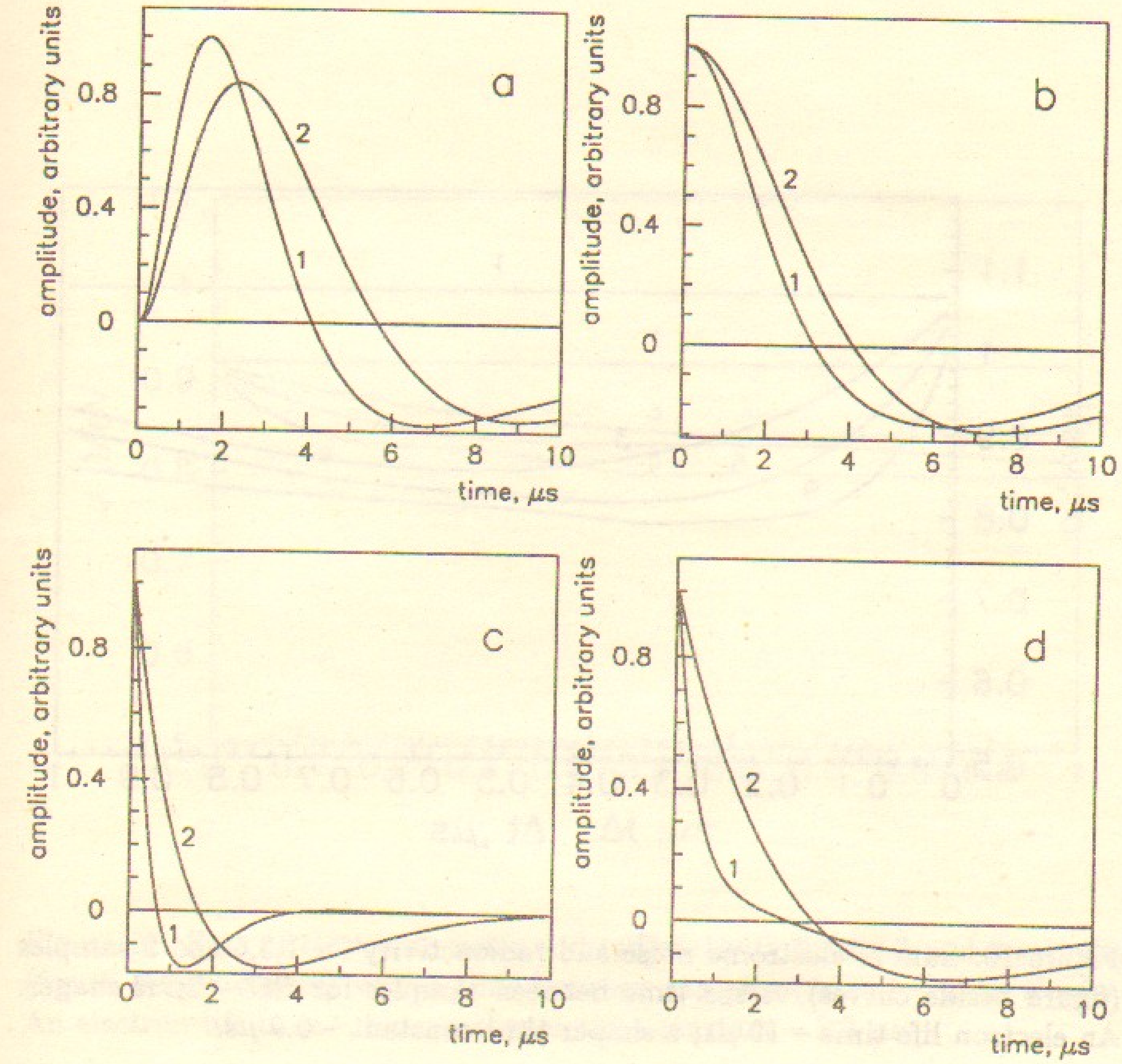

Figure 9. A waveform of useful signal (a), autocorrelation functions of radioactivity (b) and electronic noise (c), common autocorrelation functions of electronic noise and radioactivity (d) for $RC-2CR$ shaper.
1–electron life time 10 μs, time constant 0.9 μs; 2–electron life time 1 μs, time constant 2.3 μs.

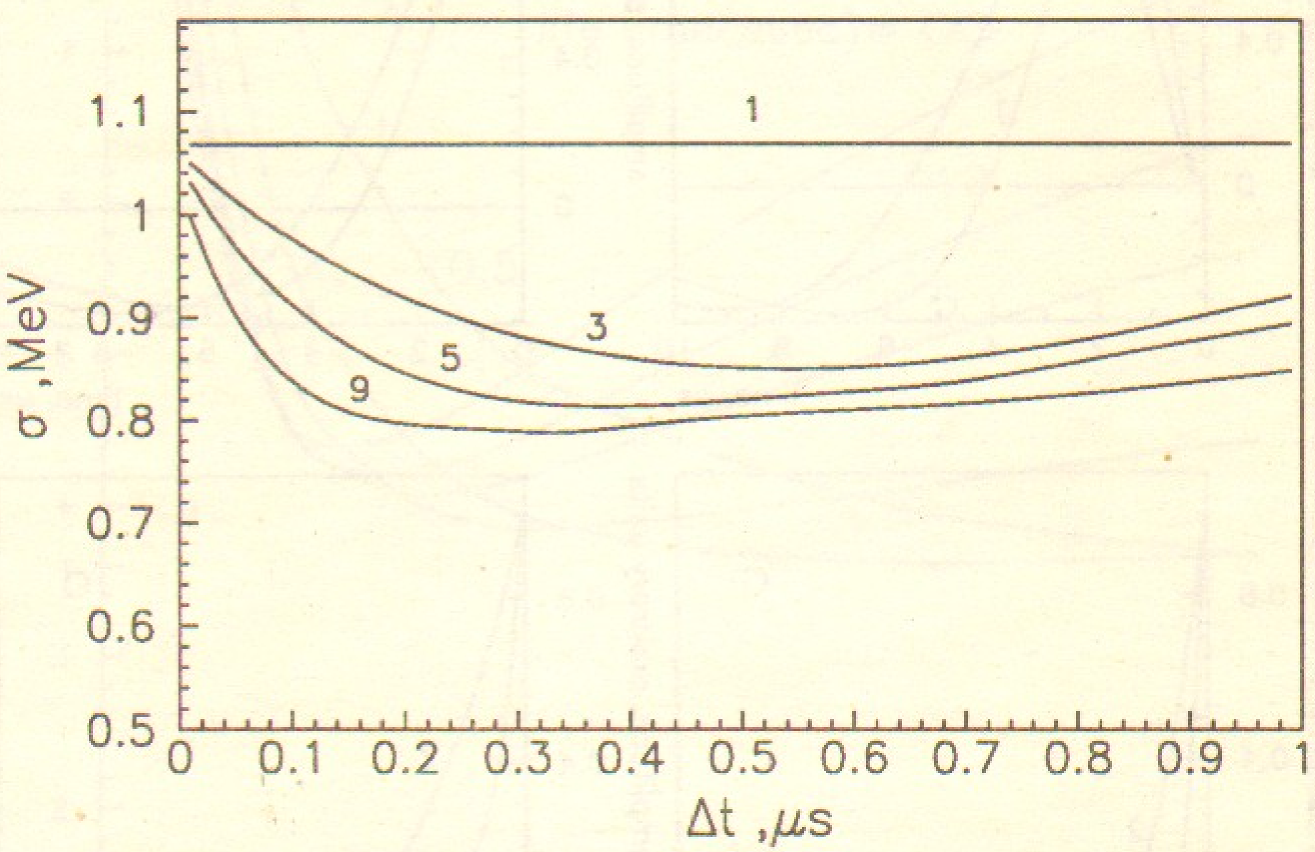

Figure 10. Sum of electronic noise and radioactivity for 1,3,5 and 9 samples (figure beside curves) versus time between samples for $RC-2CR$ shaper. An electron life time – 10 μs; a shaper time constant – 0.9 μs.

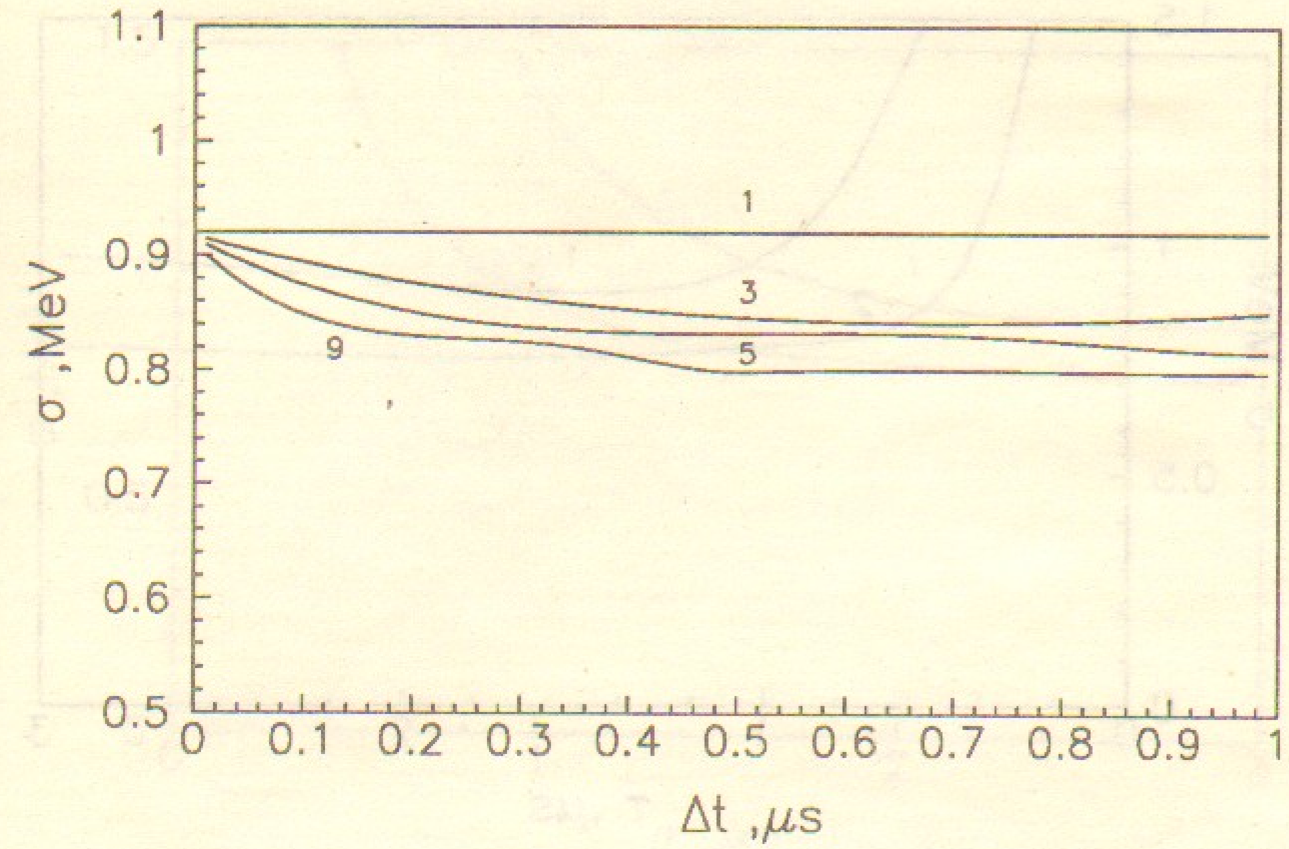

Figure 11. Sum of electronic noise and radioactivity for 1,3,5 and 9 samples (figure beside curves) versus time between samples for $RC-2CR$ shaper. An electron life time – 1 μs; a shaper time constant – 2.3 μs.

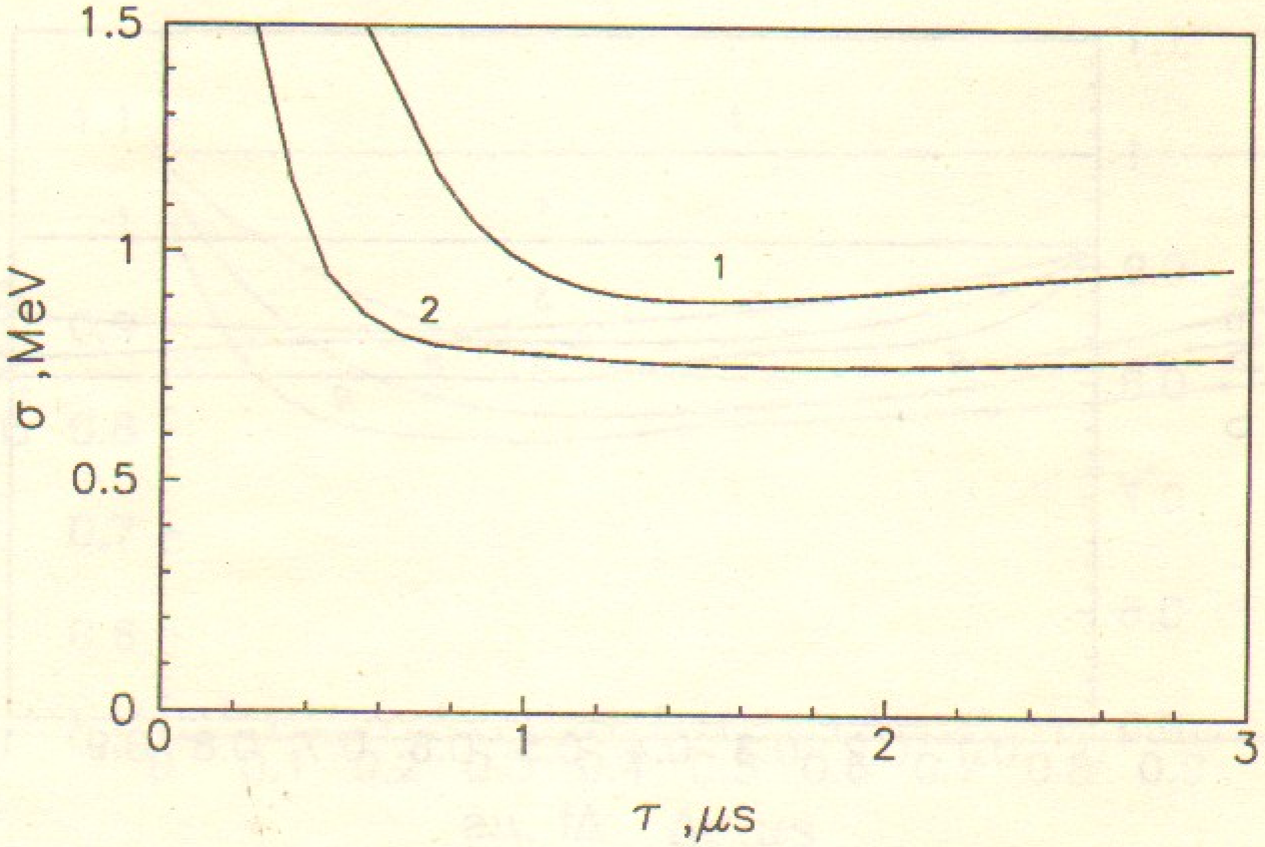

Figure 12. Sum of electronic noise and radioactivity for one (1) and 9 (2) samples versus a time constant of $RC-2CR$ shaper. An electron life time – 10 μs.

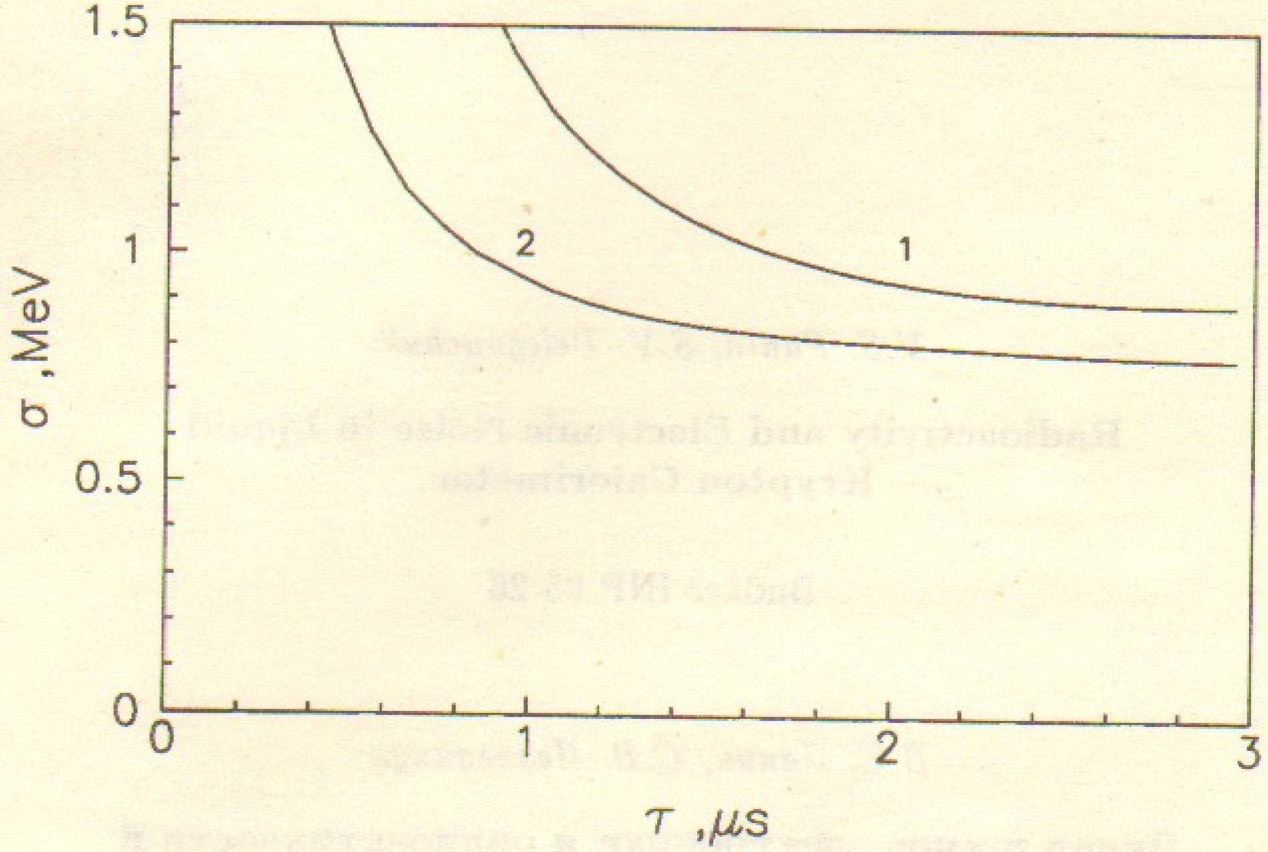

Figure 13. Sum of electronic noise and radioactivity for one (1) and 9 (2) samples versus a time constant of $RC-2CR$ shaper. An electron life time – 1 μs.